

Bistability, Probability Transition Rate and First-Passage Time in an Autoactivating Positive-Feedback Loop

Xiu-Deng Zheng^{1,3}, Xiao-Qian Yang², Yi Tao^{1*}

1 Key Laboratory of Animal Ecology and Conservational Biology, Centre for Computational and Evolutionary Biology, Institute of Zoology, Chinese Academy of Sciences, Beijing, People's Republic of China, **2** School of Mathematical Sciences, Beijing Normal University, Beijing, People's Republic of China, **3** Graduate University of the Chinese Academy of Sciences, Beijing, People's Republic of China

Abstract

A hallmark of positive-feedback regulation is bistability, which gives rise to distinct cellular states with high and low expression levels, and that stochasticity in gene expression can cause random transitions between two states, yielding bimodal population distribution (Kaern et al., 2005, *Nat Rev Genet* 6: 451–464). In this paper, the probability transition rate and first-passage time in an autoactivating positive-feedback loop with bistability are investigated, where the gene expression is assumed to be disturbed by both additive and multiplicative external noises, the bimodality in the stochastic gene expression is due to the bistability, and the bistability determines that the potential of the Fokker-Planck equation has two potential wells. Our main goal is to illustrate how the probability transition rate and first-passage time are affected by the maximum transcriptional rate, the intensities of additive and multiplicative noises, and the correlation of additive and multiplicative noises. Our main results show that (i) the increase of the maximum transcription rate will be useful for maintaining a high gene expression level; (ii) the probability transition rate from one potential well to the other one will increase with the increase of the intensity of additive noise; (iii) the increase of multiplicative noise strength will increase the amount of probability in the left potential well; and (iv) positive (or negative) cross-correlation between additive and multiplicative noises will increase the amount of probability in the left (or right) potential well.

Citation: Zheng X-D, Yang X-Q, Tao Y (2011) Bistability, Probability Transition Rate and First-Passage Time in an Autoactivating Positive-Feedback Loop. *PLoS ONE* 6(3): e17104. doi:10.1371/journal.pone.0017104

Editor: Giuseppe Chirico, University of Milano-Bicocca, Italy

Received: September 12, 2010; **Accepted:** January 20, 2011; **Published:** March 21, 2011

Copyright: © 2011 Zheng et al. This is an open-access article distributed under the terms of the Creative Commons Attribution License, which permits unrestricted use, distribution, and reproduction in any medium, provided the original author and source are credited.

Funding: This research was supported by the “Hundred Talent Program of Chinese Academy of Sciences” (A0790). The funders had no role in study design, data collection and analysis, decision to publish, or preparation of the manuscript.

Competing Interests: The authors have declared that no competing interests exist.

* E-mail: yitao@ioz.ac.cn

Introduction

Bistability arises within a wide range of biological systems from the bacteriophage λ to cellular signal transduction pathways in mammalian cells [1,2]. As a fundamental behavior of biological system, bistability has been studied extensively through experiments, theoretical analysis and numerical simulations. Hasty et al. [3] considered a single network derived from bacteriophage λ and constructed a two-parameter deterministic model describing the temporal evolution of the concentration of λ repressor protein. They showed how additive and multiplicative external noise can be used to regulate gene expression. In the case with only additive noise, they demonstrated the utility of such control through the concentration of protein switch, whereby protein production is turned “on” and “off” by using short noise pulse. In the case with multiplicative noise, they showed that small deviations in the transcription rate can lead to large fluctuations in the production of protein. Combining theory and experiments, Isaacs et al. [4] investigated the dynamics of an isolated genetic module, an *in vivo* autoregulatory gene network. As predicted by their theoretical model, temperature-induced protein destabilization led to the existence of two expression states. The result of Isaacs et al. shows clearly the effects of varying the strength of feedback activation on population heterogeneity (see also [5]). Recently, Acar et al. [6] experimentally explored how switching affects population growth by using the galactose utilization network of *Saccharomyces cerevisiae*.

Kaern et al. [2] pointed out that a hallmark of positive-feedback regulation is bistability, which gives rise to distinct cellular states with high and low expression levels, and that stochasticity in gene expression can cause random transitions between the two states, yielding bimodal population distributions (see also [7–9]). So, for the positive-feedback regulation with bistability, a challenging question is how to determine probability transition rates between the two states, or how the random transitions between the two states are affected by the transcription rate and noise strength. In this paper, a simple theoretical model for an autoactivating positive-feedback loop is investigated. Our main goal is to provide a theoretical analysis for the probability transition rate and first-passage time in the system with external noise. The paper is organized as follows. In section 2, the basic model and its bistability is presented. The analysis of the probability transition rate and first-passage time for the situations with additive and multiplicative external noises are given in section 3.

Results

Basic model

It is well known that the simplest circuit motif able to exhibit multiple stable states is the autoactivating positive-feedback loop [5,9–11], in which a single gene encodes a protein (activator), and the activator monomers bind into dimers that subsequently bind to the upstream regulatory site of the gene, activating production of

the activator monomers (see Figure 1). For example, the autoactivation of CI protein by the P_{RM} promoter of phage λ [4]. The autoactivating positive-feedback loop is expected to exhibit bistability for the protein synthesis level, i.e., a higher level and a low level of protein concentration [2,9]. Let $x(t)$ and $y(t)$ denote the concentrations of mRNA and activator protein at time t , respectively. Then, in general the macroscopic rate equation for $x(t)$ and $y(t)$ can be expressed as

$$\begin{aligned}\frac{dx}{dt} &= F(y) - \gamma_R x, \\ \frac{dy}{dt} &= Kx - \gamma_P y,\end{aligned}\quad (1)$$

where $F(y)$ represents the mRNA transcription rate, which is defined as a function of activator protein concentration with $dF(y)/dy > 0$, the parameter K denotes the translation rate, and the parameters γ_R and γ_P are the degradation rates of mRNA and protein, respectively, with $\gamma_R \gg \gamma_P$, i.e., the concentration of mRNA is a fast variable compared with the concentration of activator protein [12,13]. For the mRNA transcription rate $F(y)$, we take it as a Hill-type function

$$F(y) = \frac{k_{\max} y^{\alpha_H}}{k_H + y^{\alpha_H}} + k_f, \quad (2)$$

where k_{\max} is the maximum transcription rate, α_H the Hill coefficient where we take $\alpha_H = 2$, k_H the Hill constant, and k_f the basal transcription rate with $k_f \ll k_{\max}$ [14]. In biology, these parameters mean that: (i) k_{\max} represents the mRNA transcription rate when the activator protein concentration is large enough; (ii) $\alpha_H = 2$ implies that the activator binding processes are considered comparatively rapid and close to equilibrium, so the concentration of activator homodimer is proportional to the square of activator monomer concentration [14]; (iii) k_H is the dissociation constant of activator dimer from the regulatory site; and (iv) k_f is the mRNA transcription rate when the activator protein concentration is very low [15].

Notice that $x(t)$ can be considered to be a fast variable compared with $y(t)$ since $\gamma_R \gg \gamma_P$. Then, Eq. 1 can be reduced as

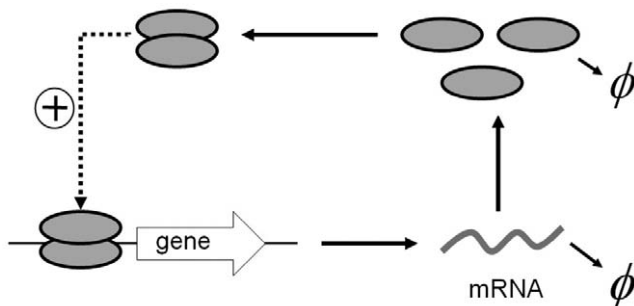


Figure 1. Modeling of autoactivating positive-feedback loop. In this model, the transcriptional activator monomers bind into dimers that bind to specific DNA sequences near the promoter, activating production of the activator monomers. The dotted line represents the positive auto-regulation. The degradation of both mRNA and protein is denoted by the slashed circle.

doi:10.1371/journal.pone.0017104.g001

$$\frac{dy}{dt} = \frac{K}{\gamma_R} \left[\frac{k_{\max} y^2}{k_H + y^2} + k_f \right] - \gamma_P y, \quad (3)$$

i.e., the fast variable can be assumed to be at an effective equilibrium, whereas the slow variable is responsible for the dynamics of the system [5,16,17]. In mathematics, one of the most important properties of Eq. 3 is its bistability, i.e., Eq. 3 has at most three fixed points, denoted by y_{s1} , y_u and y_{s2} with $y_{s1} < y_u < y_{s2}$. For the stability of y_{s1} , y_{s2} and y_u , it is easy to see that both y_{s1} and y_{s2} are locally asymptotically stable and y_u is unstable since $(K/\gamma_R)dF(y_{s_i})/dy < \gamma_P$ for $i=1,2$ and $(K/\gamma_R)dF(y_u)/dy > \gamma_P$ (see also [15]).

In biology, we are more interested in how the dynamic properties of Eq. 3 is affected by the maximum transcription rate k_{\max} (see also [15]). The relationship between the bistability and k_{\max} is plotted in Figure 2 (i.e. $\log y$ vs. k_{\max} for $dy/dt=0$) where, following Smolen et al. [15], the parameters are taken as $K = 10 \text{ h}^{-1}$, $k_f = 0.1 \text{ h}^{-1}$, $\gamma_R = 10 \text{ h}^{-1}$, $\gamma_P = 1 \text{ h}^{-1}$ and $k_H = 10$ (see also [16]) (in this paper, we keep these parameters to be fixed). Clearly, for the stability of Eq. 3, the parameter k_{\max} has two bifurcation values, denoted by k'_{\max} and k''_{\max} , respectively, with $k'_{\max} < k''_{\max}$ (where $k'_{\max} \approx 6.11 \text{ h}^{-1}$ and $k''_{\max} \approx 25.10 \text{ h}^{-1}$), i.e., the bistability exists if k_{\max} is in the interval $k'_{\max} < k_{\max} < k''_{\max}$. For the situation with $k_{\max} < k'_{\max}$ (or $k_{\max} > k''_{\max}$), the system will be monostable, i.e., the system has only one fixed point y_{s1} (or y_{s2}) if $k_{\max} < k'_{\max}$ (or if $k_{\max} > k''_{\max}$). On the other hand, if $k_{\max} = k'_{\max}$ (or $k_{\max} = k''_{\max}$), then the system will have two fixed points y_{s1} and y_u (or y_u and y_{s2}), i.e., if k_{\max} exactly equal its bifurcation value, then Eq. 3 will have two fixed points, in which one is stable and the other semi-stable.

Similar to Hasty et al. [3], we here consider also how the dynamics of protein concentration is affected by the additive and multiplicative external noises. As discussed above, if the bistability exists, then in the absence of noise, the system state will evolve identically to one of the two fixed points. The presence of a noise source will lead to the fluctuation of the system state. Hasty et al. [3] pointed out that an additive noise source alters the

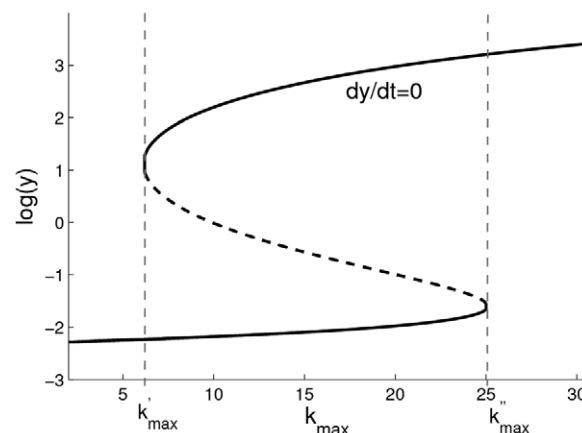


Figure 2. Bifurcation analysis of bistability in the deterministic gene expression as a function of k_{\max} . The parameters K , k_f , γ_R , γ_P and k_H are taken as $K = 30 \text{ h}^{-1}$, $k_f = 0.1 \text{ h}^{-1}$, $\gamma_R = 30 \text{ h}^{-1}$, $\gamma_P = 1 \text{ h}^{-1}$ and $k_H = 10$ (see also the main text). The bistability exists if $k'_{\max} < k_{\max} < k''_{\max}$, where $k'_{\max} \approx 6.11 \text{ h}^{-1}$ and $k''_{\max} \approx 25.10 \text{ h}^{-1}$. If $k_{\max} < k'_{\max}$ (or $k_{\max} > k''_{\max}$), then the system will be monostable (see also Ref. [14]).

doi:10.1371/journal.pone.0017104.g002

“background” protein production. This means that we need to consider the effect of a randomly varying external field on the biochemical reactions. For example, To et al. [18] provided an experiment evident to show that the change of the external noise can induce bimodality in positive transcriptional feedback loops without bistability. On the other hand, Hasty et al. [3] also pointed out that although transcription is represented by a single biochemical reaction, it is actually a complex sequence of reactions, and it is natural to assume that this part of the gene regulatory sequence is likely to be affected by fluctuations of many internal or external parameters. This implies that the transcription rate can be also considered to be a random variable.

In our model, the additive noise, denoted by $\xi(t)$, alters the “background” protein production, and is defined as a white noise with $\langle \xi(t) \rangle = 0$ and $\langle \xi(t)\xi(t') \rangle = 2D_A\delta(t-t')$ where D_A measures the level of additive noise strength. The multiplicative noise alters the transcription rate. We vary the transcription rate by allowing the parameter k_{\max} to vary stochastically, i.e., let $k_{\max} = k_{\max} + \eta(t)$, where $\eta(t)$ is also a white noise with $\langle \eta(t) \rangle = 0$ and $\langle \eta(t)\eta(t') \rangle = 2D_M\delta(t-t')$ where D_M measures the level of multiplicative noise strength. Here a natural question is whether the additive and multiplicative noises are statistically correlated. However we could imagine the correlation arising from the feedback regulation, i.e. the transcription rate (affected by noise) is chemically coupled to the protein concentration (also affected by noise). We define that the cross-correlation of $\xi(t)$ and $\eta(t)$ is $\langle \xi(t)\eta(t') \rangle = 2\mu(D_AD_M)^{1/2}\delta(t-t')$ where μ is the cross-correlation intensity [19]. In fact, for the cross-correlation between the additive noise $\xi(t)$ and multiplicative noise $\eta(t)$, we have no experimental evidence that indicate that the parameter μ should be positive, or negative. We also noticed that in a previous model developed by Hasty et al. [3], the effect of the cross-correlation between the additive and multiplicative noises on the stochastic gene expression is ignored. Thus, for the effect of μ we will only provide some theoretical possibilities.

According to the above definitions about $\xi(t)$ and $\eta(t)$, the Langevin equation corresponding to Eq. 3 is given by

$$\frac{dy}{dt} = g(y) + h(y)\eta(t) + \xi(t), \quad (4)$$

where

$$g(y) = \frac{K}{\gamma_R} \left[\frac{k_{\max} y^2}{k_H + y^2} + k_f \right] - \gamma_P y, \quad (5)$$

$$h(y) = \frac{K}{\gamma_R} \cdot \frac{y^2}{k_H + y^2}.$$

Let $\phi(y, t)$ denote the probability density distribution that the concentration of activator protein exactly equals y at time t . Then, from Risken [20], the Fokker-Planck equation of $\phi(y, t)$ corresponding to Eq. 4 can be given by

$$\begin{aligned} \frac{\partial \phi(y, t)}{\partial t} = & -\frac{\partial}{\partial y} \left[g(y) + D_M h'(y) h(y) + \mu(D_AD_M)^{1/2} h'(y) \right] \phi(y, t) \\ & + \frac{\partial^2}{\partial y^2} \left[D_A + 2\mu(D_AD_M)^{1/2} h(y) + D_M h^2(y) \right] \phi(y, t). \end{aligned} \quad (6)$$

The stationary distribution is $\phi(y) = Ce^{-U_{FP}(y)}$ where C is the normalized constant and

$$\begin{aligned} U_{FP}(y) = & \ln \left[D_A + 2\mu(D_AD_M)^{1/2} h(y) + D_M h^2(y) \right] \\ & - \int^y \frac{g(s) + D_M h'(s) h(s) + \mu(D_AD_M)^{1/2} h'(s)}{D_A + 2\mu(D_AD_M)^{1/2} h(s) + D_M h^2(s)} ds \\ = & \frac{1}{2} \ln \left[D_A + 2\mu(D_AD_M)^{1/2} h(y) + D_M h^2(y) \right] \\ & - \int^y \frac{g(s)}{D_A + 2\mu(D_AD_M)^{1/2} h(s) + D_M h^2(s)} ds \end{aligned} \quad (7)$$

is called the potential of the Fokker-Planck equation.

Additive noise

In this subsection, we consider only the effect of additive noise on the bistability, and assume that $D_M = 0$ (i.e. we here ignore the multiplicative noise). Clearly, for $D_M = 0$, Eq. 6 can be reduced to

$$\frac{\partial \phi(y, t)}{\partial t} = -\frac{\partial}{\partial y} g(y) \phi(y, t) + D_A \frac{\partial^2}{\partial y^2} \phi(y, t), \quad (8)$$

and Eq. 7 can be rewritten as

$$U_{FP}(y) = \frac{1}{2} \ln D_A - \int^y \frac{g(s)}{D_A} ds \quad (9)$$

with $U'_{FP}(y) = -g(y)/D_A$. The stationary solution of Eq. 8 is $\phi(y) = CD_A^{-1/2} e^{\int^y (g(s)/D_A) ds}$ where $C = (D_A^{-1/2} \int_0^\infty e^{\int^y (g(s)/D_A) ds} dy)^{-1}$. Obviously, $\phi(y)$ is a bimodal distribution if $k'_{\max} < k_{\max} < k''_{\max}$, i.e., stationary distribution $\phi(y)$ has two peaks corresponding to the two stable points y_{s1} and y_{s2} , respectively. This also implies that the stable point y_{si} ($i=1,2$) must correspond to the local minimum of the potential $U_{FP}(y)$, and the unstable point y_u to the local maximum of $U_{FP}(y)$. In physics, the local minimum of $U_{FP}(y)$ corresponding to y_{s1} (or y_{s2}) is also called the potential well, and the local maximum of $U_{FP}(y)$ corresponding to y_u the potential barrier [20]. Thus, for convenience we call the potential well corresponding to y_{s1} (or y_{s2}) the left (or right) well.

The depth of the right well is defined as $d_+ = U_{FP}(y_u) - U_{FP}(y_{s2})$, and, similarly, the depth of the left well is $d_- = U_{FP}(y_u) - U_{FP}(y_{s1})$. The depth of the potential well varies as the function of k_{\max} where we take the parameters $K, k_f, \gamma_R, \gamma_P$ and k_H to be fixed. The bistable potential $U_{FP}(y)$ is plotted in Figure 3A for two different k_{\max} values, where $d_- > d_+$ (solid curve) with $k_{\max} = 6.4 h^{-1}$ and $d_- < d_+$ (dotted curve) with $k_{\max} = 6.8 h^{-1}$. This strongly implies that the depth of left well decreases with the increase of k_{\max} but the depth of right well increases with the increase of k_{\max} . The relationship between the depth of potential well and k_{\max} is plotted in Figure 3B, i.e. the system state should be more easily attracted by the left well with the increase of the maximum transcription rate. It is also easy to see that there must exist a k_{\max} value such that $d_- = d_+$ (in Figure 3B, $d_- = d_+$ if $k_{\max} = 6.5861 h^{-1}$).

The effects of D_A and k_{\max} on the stationary distribution are plotted in Figure 4. We show that the decrease of D_A will increase the total probability in the left well if $k_{\max} < 6.5861 h^{-1}$ (with $d_- > d_+$) and the total probability in the right well if $k_{\max} > 6.5861 h^{-1}$ (with $d_- < d_+$). The stationary distribution $\phi(y)$ with $d_- > d_+$ ($k_{\max} < 6.5861 h^{-1}$), $d_- = d_+$ ($k_{\max} = 6.5861 h^{-1}$) and $d_- < d_+$ ($k_{\max} > 6.5861 h^{-1}$) are plotted in Figure 4A, 4B and 4C, respectively. We noticed

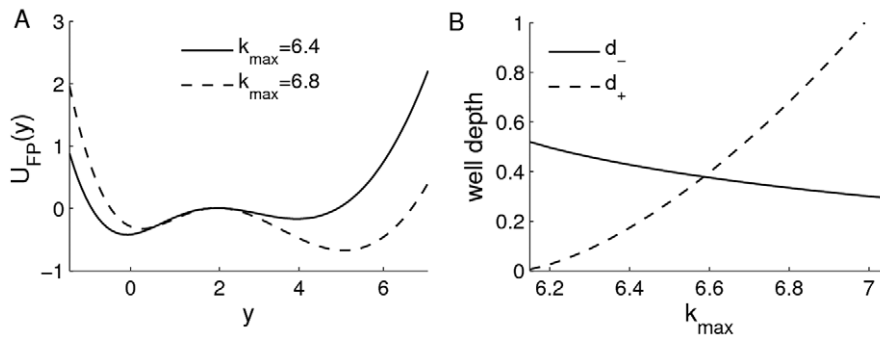


Figure 3. Effect of k_{\max} on the potential $U_{FP}(y)$. **A)** The potential for different k_{\max} values, where $d_- > d_+$ (solid curve) with $k_{\max} = 6.4 h^{-1}$ and $d_- < d_+$ (dotted curve) with $k_{\max} = 6.8 h^{-1}$. **B)** The relationship between the depth of potential well and k_{\max} . When $k_{\max} = 6.5861 h^{-1}$, both right and left potential wells have the same depth, i.e., $d_- = d_+$.
doi:10.1371/journal.pone.0017104.g003

that this result has been used to explain how the external noise can be used to control the level of protein synthesis [2,3]. For example, Hasty et al. investigated the autoregulation of bacteriophage λ repressor expression network which contains three operator sites known as OR1, OR2, and OR3 and constructed a two-parameter deterministic model describing the temporal evolution of the concentration of λ repressor protein [3]. They showed how the bistable regime is enhanced with the addition of the first operator site in the promoter region through comparing two models with only the last two operator sites and the full operator regions, respectively. They also showed how external noise can be used to regulate expression through adding external additive noise or multiplicative noise using the stochastic simulations. For the case with additive noise, they demonstrated the utility of such control through the successful switch of the concentration of a protein, whereby protein production is turned “on” and “off” by using short noise pulses, where the short noise pulse means that the noise of the system is rapidly increased to a high level in a short period of time, and after this pulse, the noise is returned to its original value.

When the system state is near the stable point y_{s_i} ($i=1,2$), the steady-state statistics of the system can be given by $\langle y \rangle = y_{s_i}$ and $\langle y^2 \rangle - \langle y \rangle^2 = -D_A/g'(y_{s_i})$ (the proof is given in Text S1) (see also [21]). This result shows clearly that when the system state is near the stable point y_{s_i} , the intensity of stochastic fluctuations around y_{s_i} is proportional to the noise strength D_A but inversely proportional to $-g'(y_{s_i})$. On the other hand, for the bistable potential function $U_{FP}(y)$, a more challenging question is how the system state jumps from one potential well to the other (i.e. the state is switches from one well to the other) because of the external noise.

Notice that the probability exchange between two potential wells occurs only near the potential barrier (i.e., at the unstable point y_u). Thus, the increase (or decrease) of the amount of probability in one potential well must result in the decrease (or increase) of the amount of probability in the other. Let $P_+(t)$ denote the total probability in the right well at time t , i.e., $P_+(t) = \int_{y_u}^{\infty} \phi(y, t) dy$, and, similarly, $P_-(t)$ the total probability in the left well at time t , i.e., $P_-(t) = \int_0^{y_u} \phi(y, t) dy$ (where we must have $P_+(t) + P_-(t) = 1$). Then the master equations of $P_+(t)$ and $P_-(t)$ can be given by

$$\frac{dP_+(t)}{dt} = -R_+ P_+(t) + R_- P_-(t),$$

$$\frac{dP_-(t)}{dt} = -R_- P_-(t) + R_+ P_+(t), \quad (10)$$

where R_+ is the probability transition rate from the right well to the left well, and R_- the probability transition rate from the left well to the right well, which are given by

$$R_+ = \frac{D_A}{2\pi} \sqrt{|U_{FP}''(y_u)| U_{FP}''(y_{s_2})} e^{U_{FP}(y_{s_2}) - U_{FP}(y_u)},$$

$$R_- = \frac{D_A}{2\pi} \sqrt{|U_{FP}''(y_{s_1})| U_{FP}''(y_u)|} e^{U_{FP}(y_{s_1}) - U_{FP}(y_u)}, \quad (11)$$

respectively, (the mathematical derivation is given in Text S1) (see also [22]). Obviously, Eq. 10 has two eigenvalues, one is $\lambda_1 = 0$, and the other $\lambda_2 = -(R_+ + R_-)$. The first one is the eigenvalue of the Fokker-Planck equation corresponding to the stationary distribution, and the latter is the lowest non-vanishing eigenvalue where $1/\lambda_2$ measures the largest time scale of the probability transition between two potential wells. From Eq. 11, we have that:

1. For both R_+ and R_- , we have $\partial R_+/\partial D_A > 0$ and $\partial R_-/\partial D_A > 0$. This means that the increase of D_A will promote the probability exchange between two wells (see Figure 5A).
2. The transition rate will decrease with the increase of the well depth, i.e., $\partial R_+/\partial d_+ < 0$ and $\partial R_-/\partial d_- < 0$ (where $d_+ = U_{FP}(y_u) - U_{FP}(y_{s_2})$ and $d_- = U_{FP}(y_u) - U_{FP}(y_{s_1})$). Hence, from Figure 3B, we have also that R_- will increase with the increase of k_{\max} but R_+ will decrease with the increase of k_{\max} . In biology, this means that the increase of k_{\max} will promote the probability transfer from the left well to the right well, or the increase of k_{\max} will be useful for maintaining a high gene expression level (see also Figure 4).
3. For convenience, we use ratio R_+/R_-

$$\frac{R_+}{R_-} = \sqrt{\frac{U_{FP}''(y_{s_2})}{U_{FP}''(y_{s_1})}} e^{-(d_+ - d_-)}. \quad (12)$$

to measure the relative intensity of probability exchange between two wells, i.e., if $R_+/R_- > 1$, then the probability is more easily

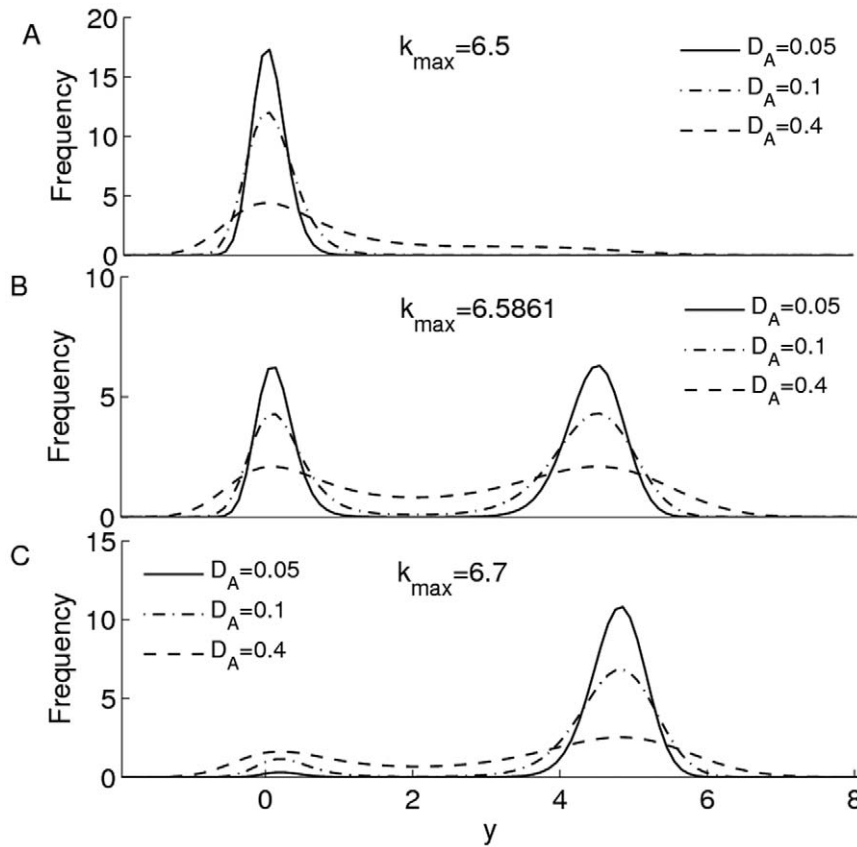


Figure 4. Effect of D_A on $\phi(y)$. The effects of additive noise strength D_A on the stationary distribution $\phi(y)$ for different k_{\max} values are plotted, where $k_{\max} = 6.5 \text{ h}^{-1}$ in **A**, $k_{\max} = 6.5861 \text{ h}^{-1}$ in **B** and $k_{\max} = 6.7 \text{ h}^{-1}$ in **C**.
doi:10.1371/journal.pone.0017104.g004

transferred from the right well to the left well, and, conversely, if $R_+/R_- < 1$, then the probability is more easily transferred from the left well to the right well. The effect of noise strength on the ratio R_+/R_- mainly depends on the difference between the depths of right and left wells (i.e., $d_+ - d_-$) since we have that $\partial(R_+/R_-)/\partial D_A > 0$ if $d_+ - d_- > 0$, and $\partial(R_+/R_-)/\partial D_A < 0$ if $d_+ - d_- < 0$. This result shows clearly that the increase of D_A will promote probability exchange from the deep well to the shallow well. The relationship between k_{\max} , D_A and R_+/R_- is plotted in Figure 5B. Clearly, the ratio R_+/R_- is an increasing function of D_A if $k_{\max} > 6.5861 \text{ h}^{-1}$ (where $d_+ > d_-$), and a decreasing function of D_A if $k_{\max} < 6.5861 \text{ h}^{-1}$ (where $d_+ < d_-$). Particularly, when $k_{\max} = 6.5861 \text{ h}^{-1}$, the ratio R_+/R_- keeps a constant (where $d_+ = d_-$), i.e., it is independent of D_A . On the other hand, it is also easy to see that the equilibrium solution of Eq. 10 must satisfy $P_-/P_+ = R_+/R_-$, i.e. $P_+ = (1 + R_+/R_-)^{-1}$ and $P_- = (R_+/R_-)(1 + R_+/R_-)^{-1}$. This shows clearly how the probabilities in the right and left wells are affected by D_A through the ratio R_+/R_- .

In physics, the first-passage time is defined as the time at which the stochastic variable first leaves a given domain [20]. In general, the first-passage time can be used to measure the robustness of the system steady-state. For our model, let τ_+ (τ_-) denote the first-passage time at which the system state first leaves the right (left) well across the potential barrier. Under the weak noise (i.e., $D_A \ll 1$), the expectations of τ_+ and τ_- can be approximated as

$$\langle \tau_+ \rangle \approx 1/R_+,$$

$$\langle \tau_- \rangle \approx 1/R_-, \quad (13)$$

respectively, and the variances of τ_+ and τ_- , denoted by V_{τ_+} and V_{τ_-} , are

$$V_{\tau_+} \approx \langle \tau_+ \rangle^2 = 1/R_+^2,$$

$$V_{\tau_-} \approx \langle \tau_- \rangle^2 = 1/R_-^2, \quad (14)$$

respectively (the mathematical derivations of Eqs 13 and 14 are given in Text S1). This strongly implies that under the weak noise, both τ_+ and τ_- should approximately obey the exponential distribution. Statistically, all transition events (called also the escape events) in a given direction (for example, from the left well to the right well, or from the right well to the left well) can be roughly considered to be independent of each other with a given average rate, i.e. the number of the transition events in a given time interval should be a Poisson process. Thus, the distribution of the first-passage time should be an exponential distribution, and its scale parameter is the inverse of the probability transition rate [23].

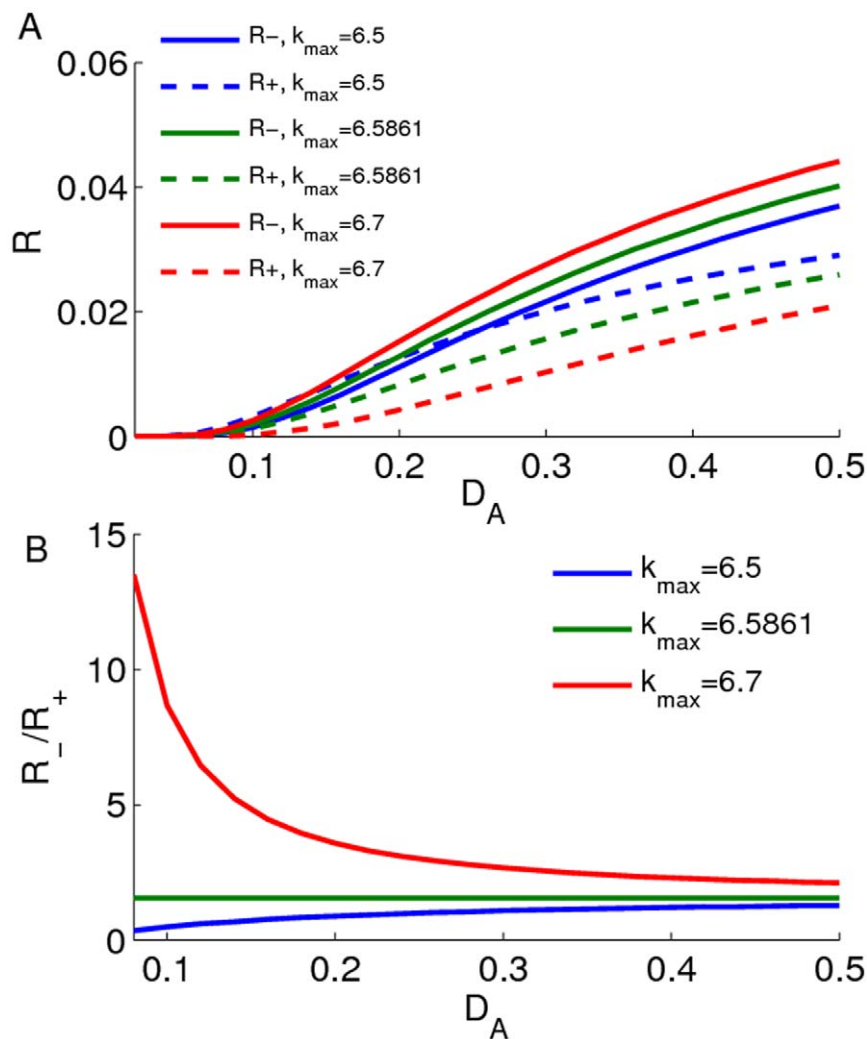


Figure 5. Effect of D_A on probability transition rate. The effects of additive noise strength D_A on both probability transition rates R_+ and R_- are shown: **A**) For different k_{\max} values, both R_+ and R_- will increase with the increase of D_A . **B**) The ratio of R_-/R_+ will increase (or decrease) with the increase of D_A if $k_{\max} < 6.5861 \text{ h}^{-1}$ (or $k_{\max} > 6.5861 \text{ h}^{-1}$). For $k_{\max} = 6.5861 \text{ h}^{-1}$, the ratio R_-/R_+ is a constant.
doi:10.1371/journal.pone.0017104.g005

The numerical simulation results for the statistical properties of τ_+ and τ_- are given in Table 1 (The simulation algorithm is given in Text S1). It is easy to see that for different D_A values (where we take $k_{\max} = 6.6 \text{ h}^{-1}$), the average of τ_+ (τ_-) (i.e. the mean first-passage time) and its standard deviation are almost same. The Monte Carlo simulations also show that under the

weak noise, the relation $\tau_+/\tau_- = (R_+/R_-)^{-1}$ is true (see Table 2). All of these simulation results exactly match the theoretical predictions.

Multiplicative noise

For $D_M \neq 0$, we first consider the situation with $\mu = 0$, i.e., $\xi(t)$ and $\eta(t)$ are independent of each other. According to this definition, we have that

Table 1. The Monte Carlo simulation results for the effect of additive noise strength D_A on the statistical properties of first passage time τ_+ and τ_- with $k_{\max} = 6.6 \text{ h}^{-1}$ (FPT: first-passage time).

D_A	$D_A = 0.05$		$D_A = 0.1$		$D_A = 0.2$		$D_A = 0.4$	
FPT	τ_-	τ_+	τ_-	τ_+	τ_-	τ_+	τ_-	τ_+
MEAN(h)	11319	28116	285.00	569.79	42.16	78.57	13.66	25.06
SD(h)	11123	27295	280.95	552.35	40.26	78.47	12.91	23.76

doi:10.1371/journal.pone.0017104.t001

Table 2. The Monte Carlo simulation results for both ratios R_-/R_+ and τ_+/τ_- with different values of D_A and $k_{\max} = 6.6 \text{ h}^{-1}$.

Ratio	$D_A = 0.05$	$D_A = 0.1$	$D_A = 0.2$	$D_A = 0.4$
R_-/R_+	2.45	2.00	1.80	1.70
τ_+/τ_-	2.48	2.00	1.86	1.83

doi:10.1371/journal.pone.0017104.t002

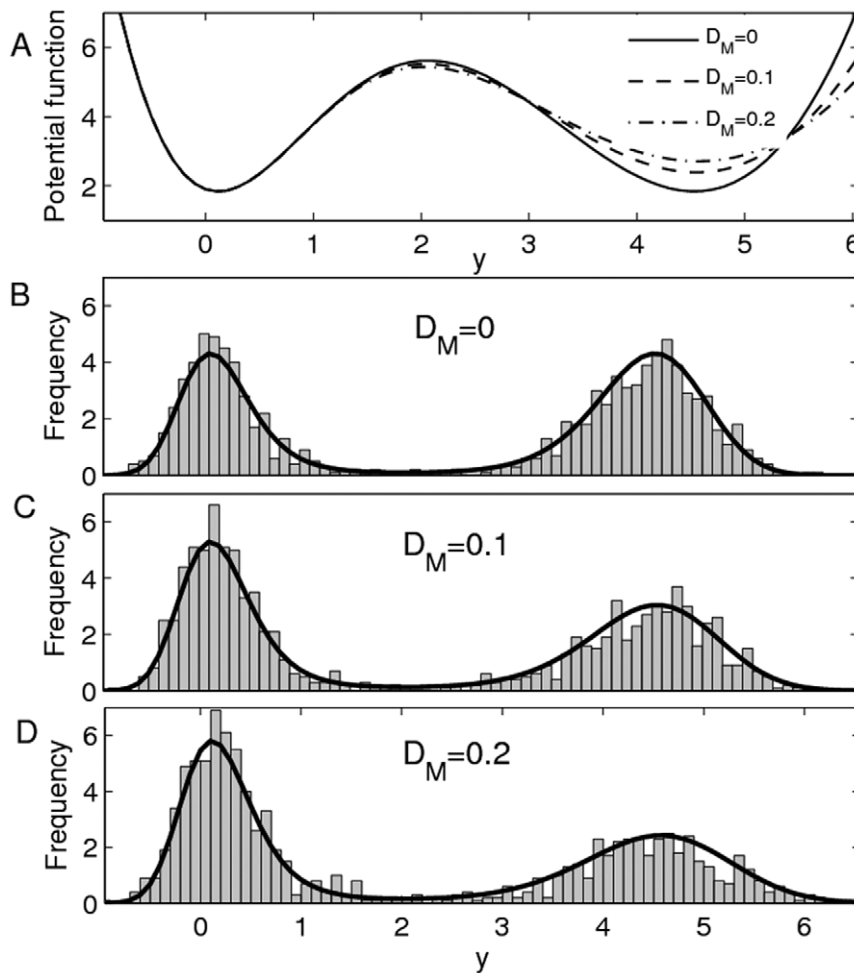


Figure 6. Effect of D_M on $U_{FP}(y)$ and $\phi(y)$. The effects of multiplicative noise strength D_M on the potential $U_{FP}(y)$ and stationary distribution $\phi(y)$ with $k_{\max} = 6.5861 \text{ h}^{-1}$ and $D_A = 0.1$ are shown: **A**) The depth of the right potential well will decrease with the increase of D_M , but the depth of the left potential well is not sensitive to the change of D_M . **B–D**) The Monte Carlo simulation results for different D_M values, i.e., $D_M = 0$ in **B**, $D_M = 0.1$ in **C** and $D_M = 0.2$ in **D**, where the solid curves denote the theoretical stationary distribution.
doi:10.1371/journal.pone.0017104.g006

$$\begin{aligned} \frac{\partial \phi(y, t)}{\partial t} = & -\frac{\partial}{\partial y} [g(y) + D_M h'(y) h(y)] \phi(y, t) \\ & + \frac{\partial^2}{\partial y^2} [D_A + D_M h^2(y)] \phi(y, t), \end{aligned} \quad (15)$$

and that

Table 3. The Monte Carlo simulation results for the effect of multiplicative noise strength D_M on the statistical properties of first passage time τ_+ and τ_- with $k_{\max} = 6.5861 \text{ h}^{-1}$ and $D_A = 0.1$.

D_M	$D_M = 0$		$D_M = 0.1$		$D_M = 0.2$		$D_M = 0.4$	
FPT	τ_-	τ_+	τ_-	τ_+	τ_-	τ_+	τ_-	τ_+
MEAN(h)	279.15	463.91	270.29	196.81	264.05	114.63	246.62	56.30
SD(h)	285.05	469.25	267.15	189.51	262.32	108.61	239.91	52.95

doi:10.1371/journal.pone.0017104.t003

$$U_{FP}(y) = \frac{1}{2} \ln [D_A + D_M h^2(y)] - \int^y \frac{g(s)}{D_A + D_M h^2(s)} ds \quad (16)$$

(see Eqs. 6 and 7). In this situation, the effect of D_M on $U_{FP}(y)$ is plotted in Figure 6A, where the parameters D_A and k_{\max} are taken as $D_A = 0.1$ and $k_{\max} = 6.5861 \text{ h}^{-1}$. In subsection 3.1, we have shown that for $D_M = 0$, both right and left wells have the same depth if $k_{\max} = 6.5861 \text{ h}^{-1}$. We will select the special value in the following analysis. We can find that the depth of the right well will decrease with the increase of D_M , but the change in the depth of the left well is very small. The stationary distribution and the Monte Carlo simulation corresponding to Figure 6A are plotted in Figure 6B–6D, respectively. These results show clearly that the amount of probability in the left (right) well will increase (decrease) with the increase of D_M .

Similar to the analysis in subsection 3.1, if both additive and multiplicative noises are weak, i.e., $D_A, D_M \ll 1$, the the expectations of the first-passage times τ_+ and τ_- can be approximated as

$$\langle \tau_+ \rangle \approx 2\pi |U_{FP}''(y_u) U_{FP}''(y_{s1})|^{-1/2} e^{U_{FP}(y_u) - U_{FP}(y_{s1})},$$

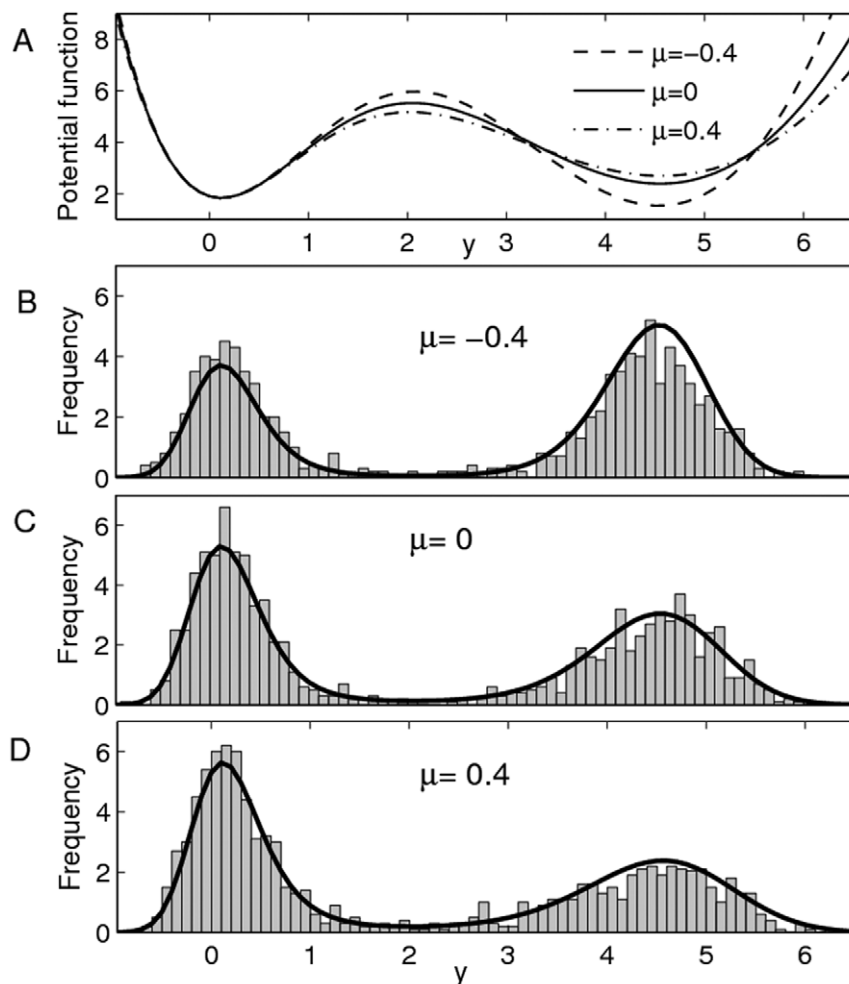


Figure 7. Effect of μ on $U_{FP}(y)$ and $\phi(y)$. The effects of μ on the potential $U_{FP}(y)$ and stationary distribution $\phi(y)$ with $k_{\max} = 6.5861 \text{ h}^{-1}$, $D_A = 0.1$ and $D_M = 0.1$ are shown: **A**) The negative (or positive) correlation between additive and multiplicative noises will increase (or decrease) the depth of the right potential well. The effect of μ on the left potential well is very small. **B–D**) The Monte Carlo simulation results for different μ values, i.e., $\mu = -0.4$ in **B**, $\mu = 0$ in **C** and $\mu = 0.4$ in **D**, where the solid curves denote the theoretical stationary distribution. Clearly, the negative (or positive) correlation will increase the probability in the right (or left) potential well.
doi:10.1371/journal.pone.0017104.g007

$$\langle \tau_- \rangle \approx 2\pi |U_{FP}''(y_u)U_{FP}''(y_{s_2})|^{-1/2} e^{U_{FP}(y_u) - U_{FP}(y_{s_2})} \quad (17)$$

(the mathematical derivation is given in Text S1) (see also [20,22]). The Monte Carlo simulation results for the statistical properties of τ_+ and τ_- are given in Table 3, in which we can find that not only both τ_+ and τ_- should obey the exponential distribution but also τ_+ is more sensitive for D_M than τ_- . This implies that the increase of the multiplicative noise strength will be useful for maintaining the protein concentration at the low level.

Secondly, for $\mu \neq 0$, we are interested in how the stochastic dynamics of the system is affected by the correlation between $\xi(t)$ and $\eta(t)$. The effect of μ on $U_{FP}(y)$ is plotted in Figure 7A where $D_A = 0.1$, $D_M = 0.1$ and $k_{\max} = 6.5861 \text{ h}^{-1}$, in which we can also find that the depth of the right well is more sensitive for the change of μ than the depth of the left well, and that if μ is negative, then the depth of the right well will increase with the increase of $|\mu|$ (i.e. absolute value of μ), and, conversely, if μ is positive, the depth of the right well will decrease with the increase of μ . The effect of μ on the stationary distribution and the Monte Carlo simulation corresponding to Figure 7A are plotted in Figure 7B–7D. It shows clearly that

the positive correlation ($\mu > 0$) will increase the amount of probability in the left well, and, conversely, the negative correlation ($\mu < 0$) will increase the amount of probability in the right well.

For the effect of μ on the first-passage time, the Monte Carlo simulation results are showed in Figure 8, in which both τ_+ and τ_- will decrease with the increase of μ , and the change rate of τ_+ is obviously larger than that of τ_- . We can also notice that the ratio τ_+/τ_- will decrease with the increase of μ (see Figure 8B). This also implies that the positive (or negative) correlation between $\xi(t)$ and $\eta(t)$ will promote the probability transition from the right (left) well to the left (right) well (see also Figure 7B–7D). Clearly, the dependence of the ratio τ_+/τ_- on μ reflects how the stationary distribution is influenced by the cross-correlation between additive and multiplicative noises, or, theoretically, the cross-correlation between $\xi(t)$ and $\eta(t)$ should be also used to control the protein synthesis.

Discussion

In this paper, the probability transition rate and first-passage time in an autoactivating positive-feedback loop with bistability are investigated. In our model, similar to Hasty et al. [3], the

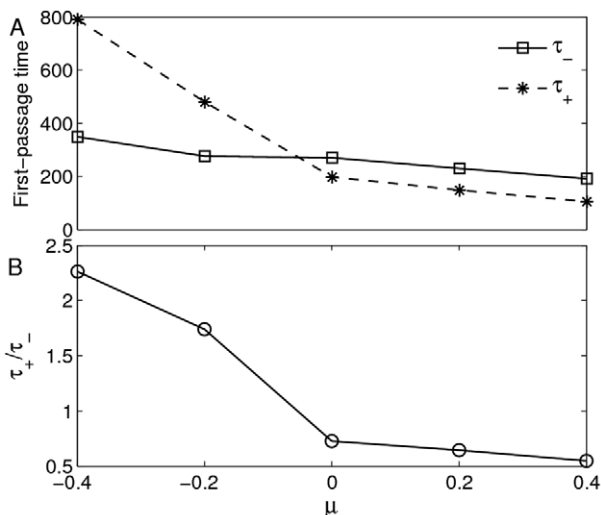


Figure 8. Effect of μ on first-passage time. The Monte Carlo simulation for the effect of μ on the first passage time τ_- , τ_+ and ratio τ_+/τ_- with $k_{\max}=6.5861 \text{ h}^{-1}$, $D_A=0.1$ and $D_M=0.1$. **A)** Both τ_- and τ_+ will decrease with the increase of μ . **B)** The ratio τ_+/τ_- also decreases with the increase of μ .
doi:10.1371/journal.pone.0017104.g008

gene expression is assumed to be disturbed by both additive and multiplicative external noises, and the bimodality in the stochastic gene expression is due to the bistability. The bistability of the deterministic dynamics Eq. 3 implies that the potential of the Fokker-Planck equation Eq. 6 has two potential wells, which correspond to the two stable points of Eq. 3, respectively, and that the stationary solution (i.e. stationary distribution) of the Fokker-Planck equation is a bimodal distribution. For our main goal, we are interested in how the system state jumps from one potential well to the other because of the external noise. In subsection 3.1, for the situation with only additive noise, our main results show that (i) both probability transition rates R_+ and R_- will increase with the increase of D_A ; (ii) R_- will increase with the increase of k_{\max} but R_+ will decrease with the increase of k_{\max} , i.e., the increase of k_{\max} will be useful for maintaining a high gene expression level; (iii) the ratio R_+/R_- measures the relative intensity of probability exchange between two potential wells, and there is a critical value of k_{\max} (which is 6.5861 h^{-1} in our case) such that the ratio R_+/R_- is an

increasing function (or a decreasing function) of D_A if k_{\max} is larger (or smaller) than the critical value; and (iv) for both first-passage times τ_+ and τ_- , if $D_A \ll 1$ (i.e. the additive noise is weak), then they obey the exponential distribution with expectations $\langle \tau_+ \rangle \approx 1/R_+$ and $\langle \tau_- \rangle \approx 1/R_-$, respectively. In subsection 3.2, for the situation with both additive and multiplicative noises, we show that (i) for $\mu=0$ (i.e. the additive noise and multiplicative noise are independent of each other), the increase of D_M will be useful for maintaining the protein concentration at the low level; and (ii) for $\mu \neq 0$, the positive (or negative) correlation between additive and multiplicative noises will promote the probability transition from the right (left) well to the left (right) well, i.e., the positive correlation will increase the amount of probability in the left potential well, and, conversely, the negative correlation will increase the amount of probability in the right potential well.

However, our results may provide some theoretical intuitions for real gene expression. For example, Hasty et al. [3] investigated the autoregulation of λ repressor expression in the lysis-lysogeny pathway in the λ virus, and they showed why the additive and multiplicative noises can be used to regulate expression (or to control the protein production). Our results further show how the probability transition between two stable states (i.e. two levels of protein synthesis) is affected, and why the cross-correlation between the additive and multiplicative external noises can be also used to regulate expression. Finally, we would like to say that the further analysis incorporating more realistic dynamics should be carried out in future studies.

Supporting Information

Text S1 Steady-state statistics, Probability transition rate, First-passage time, Method for stochastic simulation.
(PDF)

Acknowledgments

The authors thank the anonymous referee for helpful suggestions on the original paper.

Author Contributions

Conceived and designed the experiments: YT XZ. Performed the experiments: XZ. Analyzed the data: XZ YT. Contributed reagents/materials/analysis tools: XZ XY. Wrote the paper: XZ YT.

References

- Hasty J, McMillen D, Isaacs F, Collins JJ (2001) Computational studies of gene regulatory networks: in numero molecular biology. *Nat Rev Genet* 2: 268–279.
- Kaern M, Elston TC, Blake WJ, Collins JJ (2005) Stochasticity in gene expression: from theories to phenotypes. *Nat Rev Genet* 6: 451–464.
- Hasty J, Pradines J, Dolink M, Collins JJ (2000) Noise-based switches and amplifiers for gene expression. *Proc Natl Acad Sci USA* 97: 2075–2080.
- Isaacs FJ, Hasty J, Cantor CR, Collins JJ (2003) Prediction and measurement of an autoregulatory genetic module. *Proc Natl Acad Sci USA* 100: 7714–7719.
- Bennett MR, Volfson D, Tsimring L, Hasty J (2007) Transient dynamics of genetic regulatory networks. *Biphasical J* 92: 3501–3512.
- Acar M, Mettetal JT, van Oudenaarden A (2008) Stochastic switching as a survival strategy in fluctuating environments. *Nature Genetics* 40: 471–475.
- Becskei A, Seraphin B, Serrano L (2001) Positive feedback in eukaryotic gene networks: cell differentiation by graded to binary response conversion. *EMBO J* 20: 2528–2533.
- Ozbudak EM, Thattai M, Lim HN, Shraiman BI, van Oudenaarden A (2004) Multistability in the lactose utilization network of *Escherichia coli*. *Nature* 427: 737–740.
- Smits WK, Kuipers OP, Veening JW (2006) Phenotypic variation in bacteria: the role of feedback regulation. *Nature Reviews Microbiology* 4: 259–271.
- Pomeroy JR, Sontag ED, Ferrell Jr. JE (2003) Building a cell cycle oscillator: hysteresis and bistability in the activation of Cdc2. *Nature Cell Biology* 5: 346–351.
- Scott M, Terence Hwa T, Ingalls B (2007) Deterministic characterization of stochastic genetic circuits. *Proc Natl Acad Sci USA* 104: 7402–7407.
- Thattai M, van Oudenaarden A (2001) Intrinsic noise in gene regulatory networks. *Proc Natl Acad Sci USA* 98: 8614–8619.
- Paulson J (2004) Summing up the noise in gene networks. *Nature* 427: 415–418.
- Rosenfeld N, Young JW, Alon U, Swain PS, Elowitz MB (2005) Gene regulation at the single-cell level. *Science* 307: 1962–1965.
- Smolen P, Baxter DA, Byrne JH (1998) Frequency selectivity, multistability, and oscillations emerge from models of genetic regulatory systems. *Am J Cell Physiol* 274: 531–542.
- Vilar JMG, Kueh HY, Barkai N, Leibler S (2002) Mechanisms of noise-resistance in genetic oscillators. *Proc Natl Acad Sci USA* 99: 5988–5992.
- Elf J, Ehrenberg M (2003) Fast evaluation of fluctuations in biochemical networks with the linear noise approximation. *Genome Res* 13: 2475–2484.
- To TL, Maheshri N (2010) Noise can induce bimodality in positive transcriptional feedback loops without bistability. *Science* 327: 1142–1145.
- Denisov SI, Vitrenko AN, Horsthemke W (2003) Nonequilibrium transitions induced by the cross-correlation of white noises. *Phys Rev E* 68: 046132.

20. Risken H (1992) *The Fokker-Planck Equation: Methods of Solution and Applications*. Berlin: Springer.
21. van Kampen NG (1992) *Stochastic Process Theory in Physics and Chemistry*. Amsterdam: North-Holland.
22. Hu G (1992) *Stochastic Forces and Nonlinear System*. Shanghai Press for Science, Technology and Education (Chinese version).
23. Papoulis A, Pillai SU (2001) *Probability, Random Variables and Stochastic Processes*. New York: McGraw-Hill.